

# Conformational flexibility facilitates self-assembly of complex DNA nanostructures

Chuan Zhang\*, Min Su†, Yu He\*, Xin Zhao†, Ping-an Fang†, Alexander E. Ribbe\*, Wen Jiang†, and Chengde Mao\*\*

\*Department of Chemistry and †Markey Center for Structural Biology and Department of Biological Sciences, Purdue University, West Lafayette, IN 47907

Edited by Hao Yan, Arizona State University, Tempe, AZ, and accepted by the Editorial Board May 28, 2008 (received for review April 23, 2008)

**Molecular self-assembly is a promising approach to the preparation of nanostructures. DNA, in particular, shows great potential to be a superb molecular system. Synthetic DNA molecules have been programmed to assemble into a wide range of nanostructures. It is generally believed that rigidities of DNA nanomotifs (tiles) are essential for programmable self-assembly of well defined nanostructures. Recently, we have shown that adequate conformational flexibility could be exploited for assembling 3D objects, including tetrahedra, dodecahedra, and buckyballs, out of DNA three-point star motifs. In the current study, we have integrated tensegrity principle into this concept to assemble well defined, complex nanostructures in both 2D and 3D. A symmetric five-point-star motif (tile) has been designed to assemble into icosahedra or large nanocages depending on the concentration and flexibility of the DNA tiles. In both cases, the DNA tiles exhibit significant flexibilities and undergo substantial conformational changes, either symmetrically bending out of the plane or asymmetrically bending in the plane. In contrast to the complicated natures of the assembled structures, the approach presented here is simple and only requires three different component DNA strands. These results demonstrate that conformational flexibility could be explored to generate complex DNA nanostructures. The basic concept might be further extended to other biomacromolecular systems, such as RNA and proteins.**

icosahedron | three-dimensional | polyhedron | cryo-EM | molecular cages

**M**olecular self-assembly provides a bottom-up approach to the preparation of nanostructures (1–3). DNA, in particular, shows great potential to be a superb molecular system (4). In the last 20 years, DNA has been explored as building blocks for nanoconstructions, including preparation of periodic and aperiodic 2D nanopatterns (5–8) and 3D polyhedra (9–14). Most of the branched DNA structures are intrinsically flexible and are not suitable building blocks for construction of well defined geometric structures. How to overcome the conformational flexibility of branched DNA structures is a major challenge in structural DNA nanotechnology. In the last decade, a series of rigid structural motifs have been successfully engineered that lead to the rapid evolution of structural DNA nanotechnology (4). However, with more experience and knowledge, it is possible to controllably introduce the conformational flexibility to prepare complex DNA nanostructures (15). In our recent study of 3D self-assembly of DNA three-point-star tiles (16), we found that DNA tetrahedra could be readily assembled, and the tetrahedra are well behaved during sample characterizations. In contrast, DNA dodecahedra and buckyballs have significantly lower assembly yields and are prone to deformation. This phenomenon can be explained by the geometrical differences of these structures. Tetrahedra consist of triangular faces, but others do not. According to tensegrity principle, triangular faces will lead to rigid structures (11, 12, 17–20). This fact prompts us to integrate the tensegrity principle into DNA self-assembly when preparing large DNA polyhedra: DNA polyhedra should contain only triangular faces. Such structures would be expected to be rigid and resistant to deformations and will have high assembly yields. To test this hypothesis, we have designed a five-point-star motif

to assemble DNA icosahedra that have 20 triangular faces and 12 five-branched vertices. With slight modification, the same motif can assemble into large molecular cages. In the latter case, the DNA tile goes an unexpected and dramatic structural change that highlights the benefit of the structural flexibility of DNA nanomotifs.

## Results and Discussion

The five-point-star motif (tile) is a previously uncharacterized DNA motif. It belongs to a family of star motifs that include three-point-star motifs (15, 21), four-point-star (cross) motifs (6, 22), and six-point-star motifs (23). In icosahedra, each five-point-star tile will correspond to a five-way branched vertex (Fig. 1). The five-point-star motif contains a 5-fold rotational symmetry that goes through the center of the motif. This rotational symmetry relates the five branches of the motif and simplifies the motif. Although the motif consists of 11 strands, there are only three types: a long, repetitive, central blue-red strand (L), five identical medium green strands (M), and five identical short peripheral black strands (S). At the center of the tile, strand L contains five identical, single-stranded loops (colored red), which determine the tile flexibility. The longer the loops are, the more flexible the tile is. At the peripheral termini of each branch of the tile, there are two complementary, single-stranded overhangs, or sticky ends. Sticky-end association between tiles will lead to large structures.

In this work, DNA self-assembly is a one-pot process. When being mixed and slowly cooled from 95°C to 23°C, individual component DNA single strands first recognize each other and assemble into individual five-point-star tiles that further assemble into icosahedra through sticky-end association between the tiles. Icosahedra are the smallest closed structure for five-point-star motif without bending DNA duplexes. DNA duplexes are quite stiff at the length scales used in this work; their bending would be energetically unfavorable. Each vertex is one star tile, and each edge is composed of two associated branches from two tiles. When designing the tiles for icosahedron structures, the following factors might be important. (i) In the content of icosahedron structure, the five-point-star tiles are not planar. Instead, all component branches will bend out of the original plane by  $\approx 32^\circ$ , and the tiles become a cone shape with a 5-fold rotational symmetry. To ensure the tiles to have enough flexibility for such a degree of bending, the central single-stranded loops (red color segments in Fig. 1) are designed to be 5 bases long. (ii) Any two adjacent vertexes are separated by two parallel duplexes, whose lengths are 42 base pairs or four turns. Because

Author contributions: C.Z., W.J., and C.M. designed research; C.Z., M.S., and Y.H. performed research; C.Z., M.S., Y.H., X.Z., P.-a.F., A.E.R., W.J., and C.M. analyzed data; and C.Z. and C.M. wrote the paper.

The authors declare no conflict of interest.

This article is a PNAS Direct Submission. H.Y. is a guest editor invited by the Editorial Board.

†To whom correspondence should be addressed at: 560 Oval Drive, West Lafayette, IN 47907. E-mail: mao@purdue.edu.

This article contains supporting information online at [www.pnas.org/cgi/content/full/0803841105/DCSupplemental](http://www.pnas.org/cgi/content/full/0803841105/DCSupplemental).

© 2008 by The National Academy of Sciences of the USA

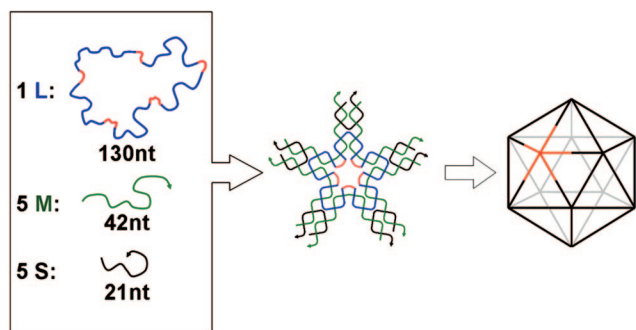


**Fig. 1.** Self-assembly of DNA icosahedra. Three different types of DNA single strands stepwise assemble into sticky-ended five-point-star motifs (tiles), which then further assemble into icosahedra. Each vertex in the icosahedra is a five-point-star tile; one of them is highlighted as golden. Note that the red colored central loops are 5 bases long.

of the helical nature of DNA duplexes, the repeating distance with integral number (here it is four) of helical turns will accumulate any curvature intrinsic to the DNA tiles in the same direction, which will promote the formation of closed complexes (6). (iii) Each sticky end consists of four G-C base pairs. The strong G-C base pairing imposes kinetic controls in the assembly process and is expected to favor closed complexes (24). It also ensures the stability of the final assemblies. (iv) Finally, a low DNA concentration (20 nM) is used to prevent large assemblies from forming.

The assembled DNA icosahedron has been characterized by multiple techniques, including native PAGE, dynamic light scattering (DLS), and cryogenic electron microscopy (cryo-EM) imaging. When a correct molecular ratio is used, only one band appears on the native PAGE, which has much slower mobility than the five-point-star tile itself (Fig. 2*A*). It suggests that the tiles assemble into a large, well defined, molecular complex. DLS studies reveal that the DNA complex has an apparent hydrodynamic radius of  $20.0 \pm 2.8$  nm (Fig. 2*B*). This value agrees well with the radius of the circumscribed sphere of the expected DNA icosahedron (19.5 nm), assuming that a DNA duplex has a pitch of 0.33 nm/base pair and a diameter of 2 nm.

To provide direct evidence of the formation of DNA icosahedra, we have imaged the DNA samples by cryo-EM (Fig. 3). Flash-freezing is likely to keep the DNA complexes in their native conformations. Most particles observed in cryo-EM images have icosahedral shapes of the expected size. The observed diameters are  $\approx 40$  nm, nicely matching the diameter of designed icosahedron (39.0 nm). With experimentally observed particles,

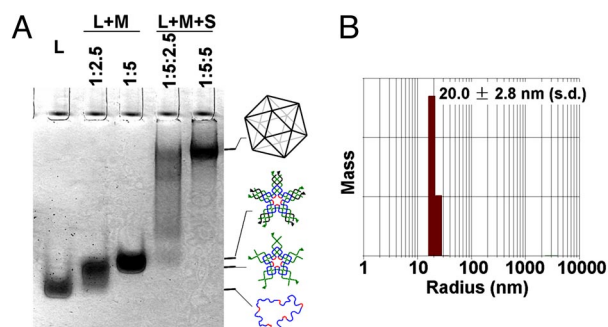


**Fig. 2.** Characterization of the self-assembled DNA icosahedron. (A) Native PAGE (2.5%) analysis. The sample compositions are indicated above the gel image, and the identity of each band is suggested on the right. (B) DLS analysis of the mass distribution along the hydrodynamic radius of the DNA complexes.

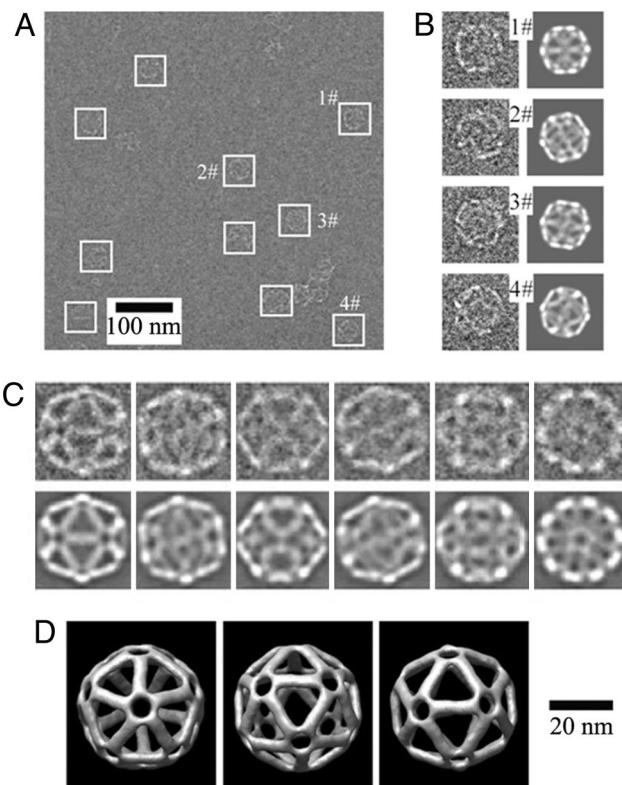


**Fig. 3.** Cryogenic transmission electron microscopy (cryo-EM) analysis of DNA icosahedron. (A) A representative raw cryo-EM image. White boxes indicate the DNA particles. (B) Comparison of raw images of individual particles at a high magnification (Left) and the corresponding computer-generated model projections (Right). (C) Comparison of class average of particle images with similar views (Upper) and the corresponding computer-generated model projections (Lower). (D) Three views of the DNA icosahedron structure reconstructed from cryo-EM images.

a DNA icosahedron structure is revealed by a technique of 3D single-particle reconstruction (25), which is a technique routinely used in studies of virus structures. The resolution of the icosahedral structure is 2.8 nm, as determined by Fourier shell correlation (25). A strong support for the reconstructed model comes from the comparison between the computed projections from model and the class averages of raw particle images with similar views [Fig. 3*C* and [supporting information \(SI\) Fig. S1](#)]. They match each other very well. Because the contrast of the DNA particles in cryo-EM is very low, it is necessary to impose the intrinsic structural symmetry (here, icosahedral symmetry) during the reconstruction to increase the resolution. Relaxed with lower symmetries (for example, C<sub>5</sub>, a 5-fold rotational symmetry), the reconstruction generates a similar structure with noisier signals (Fig. S2). It confirms that the assembled DNA complexes indeed have the icosahedral structure.

DNA icosahedra are a class of interesting structures for their rigid geometry, high symmetry, and resemblance to spherical viral capsids. Different potential strategies have been proposed. For example, based on his recently developed concept of “DNA origami”, Paul Rothmund (26) has proposed the use of many DNA short strands to fold thousands-bases-long single DNA strands (i.e., M13 genomic DNA) into polyhedra. The idea is very interesting; however, its experimental realization remains elusive. The current work represents a successful assembly of DNA icosahedra. Moreover, the 3D DNA objects in most previous reports (9–13) are highly symmetrical in terms of DNA backbones but are not symmetrical when the DNA sequences are



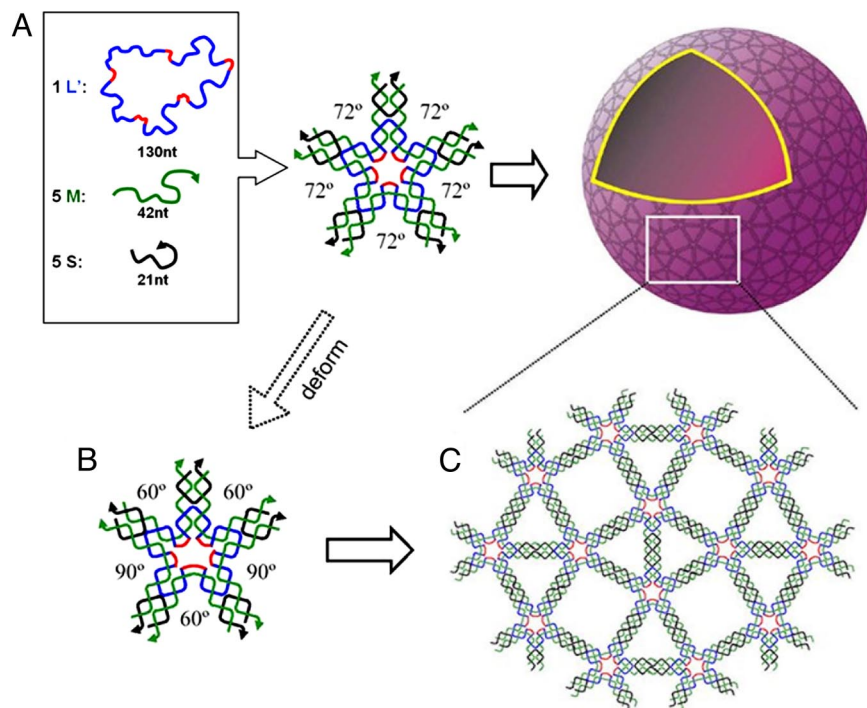


**Fig. 5.** Proposed assembly process of DNA five-point-star tiles at high DNA concentrations. On the surface of the assembled DNA nanocages, DNA tiles are arranged into tetragonal 2D crystals. Compared with the free-DNA five-point-star tile, the branches in the final structure have asymmetrical bends in the molecular plane. The angles between two neighboring branches varies (three 60° and two 90°) in the final structure and are all different from the angle (72°) in the free tiles.

EDTA, and 12.5 mM magnesium acetate. The icosahedron were assembled from strands L, M, and S at DNA concentration of 20 nM (in terms of DNA tiles); large DNA cages were assembled from strands L', M, and S at DNA concentration of 1  $\mu$ M. DNA assembly involved cooling solutions from 95°C to room temperature ( $\approx$ 23°C) over 48 h. After assembly, the DNA samples were then directly used for AFM imaging and DLS studies. For cryo-EM imaging of the icosahedron, the sample was concentrated to  $\approx$ 2  $\mu$ M with Microcon YM-30 (30 kDa) Centrifugal Filter Units before flash-freezing.

**Nondenaturing PAGE.** Nondenaturing gels containing polyacrylamide (19:1 acrylamide/bisacrylamide) were run on a FB-VE10-1 electrophoresis unit (FisherBiotech) at 4°C (80 V, constant voltage). The running buffer was TAE/Mg<sup>2+</sup> buffer. Before electrophoresis, the DNA samples were concentrated with Microcon YM-30 (30 kDa) Centrifugal Filter Units to  $\approx$ 200 nM if the sample concentrations were <200 nM. After electrophoresis, the gels were stained with Stains-All (Sigma) and scanned.

**AFM Imaging.** A drop of 1.5  $\mu$ l of DNA solution was spotted onto freshly cleaved mica surface (Ted Pella, Inc.), and incubated for 10 s to allow DNA to absorb onto the substrate. Then 50  $\mu$ l of TAE/Mg<sup>2+</sup> buffer was placed on the top of the DNA sample. The imaging was performed at 23°C in tapping mode on a Multimode AFM with Nanoscope IIIa controller (Veeco) with NP-5 tips (Veeco) in a fluid cell. The tip-surface interaction was minimized by optimizing the scan set-point to the highest possible value.

**DLS.** DNA sample solutions (12  $\mu$ l) were measured by DynaPro 99 (Protein Solutions/Wyatt) with laser wavelength of 824 nm at 23°C.

**Cryo-EM Imaging.** A drop of 3  $\mu$ l of concentrated DNA solution was pipetted onto a Quantifoil grid. Then, the grid was blotted and immediately plunge-

frozen into ethane slush cooled by liquid nitrogen. The data were recorded by using a Gatan 4 k  $\times$  4 k CCD camera in a Philips CM200 transmission electron microscope with field-emission gun operating at 200 kV accelerating voltage. To enhance the image contrast, underfocuses in the range of 2–4  $\mu$ m were used to record the images. The calibrated magnification used for DNA icosahedrons was  $\times$ 52,260, resulting in pixel sizes of 2.87 Å.

**Single-Particle Reconstruction.** Three-dimensional reconstructions of the DNA icosahedron used the single-particle image-processing software EMAN (25). The initial models were built by using 100 randomly selected raw particles. The initial orientation of individual particles was randomly assigned within the corresponding asymmetry unit of the icosahedron. Eight hundred eighty-four particles were used for the single-particle reconstruction. Ninety-nine reference projections in the icosahedron asymmetric unit were generated in the icosahedral asymmetric unit with an angular interval of 2°. A projection-matching algorithm was then used to determine the center and orientation of raw particles in the iterative refinement. The icosahedron symmetry was imposed during the reconstruction. The map resolution was determined to be at 2.8 nm by using the Fourier shell correlation (0.5 threshold criterion) of two 3D maps independently built from half datasets. Control reconstructions without imposing any symmetry or with lower symmetries imposed were performed to check that particles indeed had the icosahedral symmetry. Final 3D maps were visualized by using UCSF Chimera software (37).

**ACKNOWLEDGMENTS.** This work was supported by National Science Foundation Grant CCF-0622093, National Institutes of Health (NIH) Grant R21EB007472, and through the NIH Roadmap for Medical Research Grant PN2EY018230. AFM and DLS studies were carried out in the Purdue Laboratory for Chemical Nanotechnology. The cryo-EM images were taken in the Purdue Biological Electron Microscopy Facility, and the Purdue Rosen Center for Advanced Computing provided the computational resource for the 3D reconstructions.

- Hamley IW (2003) Nanotechnology with soft materials. *Angew Chem Int Ed* 42:1692–1712.
- Lehn JM (2002) Toward complex matter: Supramolecular chemistry and self-organization. *Proc Natl Acad Sci USA* 99:4763–4768.
- Reinhoudt DN, Crego-Calama M (2002) Synthesis beyond the molecule. *Science* 295:2403–2407.
- Seeman NC (2003) DNA in a material world. *Nature* 421:427–431.
- Winfree E, Liu FR, Wenzler LA, Seeman NC (1998) Design and self-assembly of two-dimensional DNA crystals. *Nature* 394:539–544.

- Yan H, Park SH, Finkelstein G, Reif JH, LaBean TH (2003) DNA-templated self-assembly of protein arrays and highly conductive nanowires. *Science* 301:1882–1884.
- Rothemund PWK (2006) Folding DNA to create nanoscale shapes and patterns. *Nature* 440:297–302.
- Rothemund PWK, Papadakis N, Winfree E (2004) Algorithmic self-assembly of DNA Sierpinski triangles. *PLoS Biol* 2:2041–2053.
- Chen JH, Seeman NC (1991) Synthesis from DNA of a molecule with the connectivity of a cube. *Nature* 350:631–633.

10. Zhang YW, Seeman NC (1994) Construction of a DNA-truncated octahedron. *J Am Chem Soc* 116:1661–1669.
11. Shih WM, Quispe JD, Joyce GF (2004) A 1.7-kilobase single-stranded DNA that folds into a nanoscale octahedron. *Nature* 427:618–621.
12. Goodman RP, et al. (2005) Rapid chiral assembly of rigid DNA building blocks for molecular nanofabrication. *Science* 310:1661–1665.
13. Aldaye FA, Sleiman HF (2007) Modular access to structurally switchable 3D discrete DNA assemblies. *J Am Chem Soc* 129:13376–13377.
14. Zimmerman J, Cebulla MPJ, Monninghoff S, von Kiedrowski G (2008) Self-assembly of a DNA dodecahedron from 20 trisiliconucleotides with C3h linkers. *Angew Chem Int Ed* 10.1002/anie.200702682.
15. He Y, Mao CD (2006) Balancing flexibility and stress in DNA nanostructures. *Chem Commun* 9:968–969.
16. He Y, et al. (2008) Hierarchical self-assembly of DNA into symmetric supramolecular polyhedra. *Nature* 452:198–201.
17. Ingber DE (1997) Tensegrity: The architectural basis of cellular mechanotransduction. *Annu Rev Physiol* 59:575–599.
18. Motro R (2006) *Tensegrity: Structural Systems for the Future* (Butterworth-Heinemann, Boston).
19. Liu D, Wang MS, Deng ZX, Walulu R, Mao CD (2004) Tensegrity: Construction of rigid DNA triangles with flexible four-arm DNA junctions. *J Am Chem Soc* 126:2324–2325.
20. Scheffler M, Dorenbeck A, Jordan S, Wustefeld M, von Kiedrowski G (1999) Self-assembly of trisiligo-nucleotidyls: The case for nano-acetylene and nano-cyclobutadiene *Angew Chem Int Edit* 38:3312–3315.
21. He Y, Chen Y, Liu HP, Ribbe AE, Mao CD (2005) Self-assembly of hexagonal DNA two-dimensional (2D) arrays. *J Am Chem Soc* 127:12202–12203.
22. He Y, et al. (2005) Sequence symmetry as a tool for designing DNA nanostructures. *Angew Chem Int Ed* 44:6694–6696.
23. He Y, Tian Y, Ribbe AE, Mao CD (2006) Highly connected two-dimensional crystals of DNA six-point-stars. *J Am Chem Soc* 128:15978–15979.
24. Ke YG, Liu Y, Zhang JP, Yan H (2006) A study of DNA tube formation mechanisms using 4-, 8-, and 12-helix DNA nanostructures. *J Am Chem Soc* 128:4414–4421.
25. Ludtke SJ, Baldwin PR, Chiu W (1999) EMAN: Semiautomated software for high-resolution single-particle reconstructions. *J Struct Biol* 128:82–97.
26. Rothmund PWK (2006) in *Nanotechnology: Science and Computation*, eds Chen JH, Jonoska N, Rozenberg G (Springer, Heidelberg), pp 3–21.
27. Casjens S (1985) *Virus Structure and Assembly* (Jones and Bartlett, Sudbury, MA).
28. Caspar DLD, Klug A (1962) Physical principles in construction of regular viruses. *Cold Spring Harb Symp* 27:1–24.
29. Twarock R, Hendrix RW (2006) Crosslinking in viral capsids via tiling theory. *J Theor Biol* 240:419–424.
30. Goodman RP, et al. (2008) Reconfigurable, braced, three-dimensional DNA nanostructures. *Nat Nanotechnol* 3:93–96.
31. Comellas-Aragones M, et al. (2007) A virus-based single-enzyme nanoreactor. *Nat Nanotechnol* 2:635–639.
32. Erben CM, Goodman RP, Turberfield AJ (2006) Single-molecule protein encapsulation in a rigid DNA cage. *Angew Chem Int Ed* 45:7414–7417.
33. Douglas T, Young M (1998) Host-guest encapsulation of materials by assembled virus protein cages. *Nature* 393:152–155.
34. Wang Q, Lin TW, Tang L, Johnson JE, Finn MG (2002) Icosahedral virus particles as addressable nanoscale building blocks. *Angew Chem Int Ed* 41:459–462.
35. Duckworth BP, et al. (2007) A universal method for the preparation of covalent protein-DNA conjugates for use in creating protein nanostructures. *Angew Chem Int Ed* 46:8819–8822.
36. Seeman NC (1990) *De novo* design of sequences for nucleic-acid structural-engineering. *J Biomol Struct Dyn* 8:573–581.
37. Goddard TD, Huang CC, Ferrin TE (2007) Visualizing density maps with UCSF Chimera. *J Struct Biol* 157:281–287.